Acta Technologica Agriculturae 3
Nitra, Slovaca Universitas Agriculturae Nitriae, 2024, pp. 179–186

POSSIBILITIES OF DETECTING AND EVALUATING THERMAL DEFECTS IN AGRICULTURAL BUILDING ENVELOPES USING SIMULTANEOUS INFRARED THERMOGRAPHY AND COMPUTER MODELLING

Petr JUNGA*, Tomáš KOUTNÝ, Zuzana TICHÁ, Jan KUDĚLKA, Jan MAREČEK

Mendel University in Brno, Faculty of AgriSciences, Department of Agricultural, Food and Environmental Engineering, Czech Republic, tomas.koutny@mendelu.cz (T.K.), zuzana.ticha@mendelu.cz (Z.T.) jan.kudelka@mendelu.cz (J.K.), jan.marecek@mendelu.cz (J.M.)

*correspondence: petr.junga@mendelu.cz

The aim of this paper is to investigate the possibility of using two different methods together to detect more accurately and to evaluate thermal defects in the envelope of agricultural buildings. The structure of heated agricultural buildings is significantly influenced by the characteristics of the indoor environment (aggressive gaseous and liquid substances, high humidity, higher heating temperatures, etc.). In this study, research has been conducted that synergistically combines two methods for the evaluation of thermal defects, where the structure is evaluated using infrared thermography and at the same time described as a numerical model for a more detailed identification of envelope defects and thermal bridges. The study confirmed that in agricultural building structures, thermal defects are most commonly found in the areas of window lintels, ceiling and bracing structures, window and door joints, and foundation and floor joints, while the proposed combination of the two methods for assessing thermal defects in structures demonstrated superior performance in terms of accuracy and detail of results obtained compared to the standard partial use of only one of these methods.

Keywords: thermogram; non-destructive testing; temperature field model; thermal irregularities; energy efficiency

Infrared thermography (IRT) is a non-destructive method used to evaluate the thermal defects of buildings envelope, typically post-construction. 2D or 3D computer modelling is used to analyse the thermal defects of structure details, typically pre-construction phase. The assessment of structural failures in the pre-construction and post-construction phase is necessary in the terms of the long-term technical life of buildings and energy savings. Thermography can be applied to the diagnosis of building energy losses, but also to the test of technical building equipment (Balaras and Argiriou, 2002; Changmin et al., 2022).

The development of mechanisation and technology has triggered the growing energy consumption in the agricultural industry. Energy saving in the agricultural industry becomes equally essential with that in the manufacturing, building, and transportation industries. The implementation of reducing energy consumption should be without costing the agricultural production, which is closely related to the food security of human beings (Chen et al., 2020).

The infrared thermography technique is widely used in the industry and agriculture sector. Other examples are also presented as a valuation of drying operation (Vitázek and Tirol, 2008), or a valuation of interior conditions and surface temperature in a heated milking house (Karas and Gálik, 2004) or for a calculation of the heat losses of boilers for biomass combustion (Vítěz and Trávníček, 2011).

One way to achieve carbon neutrality is by improving the energy performance of existing buildings, which requires accurate measurements. In particular, an accurate measurement of heat loss coefficient is critical because a building envelope is an important parameter of the energy performance analysis (Kim et al., 2022).

A study analysing the efficiency of a solar water heating system, potential financial savings, and investment profitability of this renewable energy source is presented by Herbut et al. (2018). The building industry is responsible for considerable energy consumption and the production of large amounts of greenhouse gas emissions world-wide. Hence, reducing the building heat losses that occur through the building envelope, especially through the floor foundations, is important (El Saied et al., 2022).

On-farm energy consumption is becoming increasingly important in the context of rising energy costs and concerns over greenhouse gas emissions (Kythreotou et al., 2012). Thermal bridges are weak points of building envelopes that can lead to energy losses, collection of moisture, and formation of mould in the building fabric. To detect thermal bridges of large building stocks, drones with thermographic cameras can be used (Mayer et al., 2023). Higher demands for energy efficiency in nearly zero energy buildings give rise to concerns on the impact of thermal bridges on building's thermal performance (Zhao et al., 2022). A significant portion of the cooling or heating load of buildings is contributed by relatively large heat flux through thermal bridges. Water vapour concentration significantly alters thermal conductivity and heat transfer characteristics within thermal bridges, affecting building energy consumption, particularly in humid climates (Xue et al., 2023). For the quantitative diagnosis of defects that cause thermal bridges through IR thermography at specific time points, changes in thermal distribution according to the window-wall joint construction level were examined in a dynamic environment. Choi et al. (2022) proposed a method to quantitatively evaluate the construction defects of the window-wall joint and identify the thermal bridge in the field.

Heading towards more energy-efficient buildings, legislative requirements are becoming increasingly demanding. The implementation of international standards in many national building codes has shown that the thermal bridge effect may significantly contribute to heat flows through building envelopes (Theodosiou et al., 2021). Thermal bridging is known to affect the thermal performance of light-weight steel-framed external walls (Kempton et al., 2021). Thermal bridges accounted for 30% of the impact on the energy performance of European residential building stock (Tejedor et al., 2020). The amount of heat loss through thermal bridges increases with the improvement of the thermal insulation performance of the building exterior wall, making thermal bridges vulnerable points of thermal insulation. The wall-to-floor thermal bridge takes the most considerable fraction on the building envelope and has the largest heat flux (Ge et al., 2021).

This paper presents the joint use of infrared thermography and computer heat transfer modelling methods for the assessment of thermal envelope failures in agricultural buildings.

Material and methods

The first analysed building is a poultry house located in the district of Brod nad Dyjí, Czech Republic. The second analysed building is an old piggery located in the district of Suchohrdly u Miroslavi (Czech Republic). The third analysed building is a farm biogas plant located in the district of Suchohrdly u Miroslavi, Znojmo (Czech Republic).

Infrared thermography measurement

The infrared thermography measurement is performed according to EN 13187 (1999). Thermal analyses were performed with a FLUKE Ti32 thermal camera FOV: 45°. Air temperature, humidity, distance from the object to be measured, and material emissivity were measured for thermal imaging. Infrared thermography works best for assessing heat spread in buildings when a minimum temperature difference of 10–15 °C between the external and internal environment is guaranteed. Air temperature and relative humidity were measured using the KIMO AMI 300 multifunction equipment. Reflected temperature was measured using a lambert reflector and was taken into account in the evaluation of thermograms. The measurement was performed in overcast sky conditions. Thermal control measurements were taken at a constant distance from the equipment being measured. Three thermograms were produced within one hour. The distance of the camera from the object to be measured was determined using the Leica DISTOtm A5 laser EDM device (measurement accuracy: ±1.5 mm at a distance between 0.2 m and 200 m). The evaluation of thermograms was performed using the Fluke SmartView software and ThermaCAM QuickReport software.

Computer heat transfer modelling

The initial step of computer modelling is the creation of a detailed 2D or 3D structural model of the analysed detail in the CAD software. From the building construction detail, a simple vector model is created, which is then used to create the actual model of temperature fields. The next step is to analyse the heat transfer across the thermal bridges, which is characterised by 2D or 3D heat flux. The modelling process continues by creating detailed thermal models of the analysed thermal bridges using the Area 2011 software. The Area 2011 software is based on the finite-element method and provides 2D heat transfer models. The boundaries of model geometry meet the requirements specified in EN ISO 10211 (2020). The individual elements of the model under consideration are assigned appropriate properties, and other conditions (in particular, boundary conditions for the parameters of the internal and external environment) are set. After all the required parameters have been entered, the numerical calculation of the temperature field is carried out with the creation of a calculation protocol and graphical outputs.

Results and discussion

Case study 1 – the poultry house

The first object for IR thermography survey is the poultry house object. Thermographic measurements were performed under the following boundary conditions: interior temperature t_i = 24 °C; exterior air temperature t_e = -0.9 °C; relative humidity 71%; the distance of the measured object 15.5 m; air velocity v_a = 0.35 m·s^{-1}; and emissivity 0.92.

In a typical thermogram shown in Fig. 1, detailed analysis areas are defined, from which surface temperature values are subsequently taken for further evaluation. The delineated areas are schematically shown in the thermogram and include the points which are under consideration with their respective temperature values. The individual areas are labelled in the thermogram and can be specified as follows: Area S1 (numerous temperature anomalies at the reinforced concrete ring beam); Area S2 (envelope with no significant temperature anomalies); Area S3 (numerous temperature anomalies at the floor structure).

Figure 1 represents the first part of the poultry house façade containing the parts of the structure with temperature deviations. The most problematic part of the structure is the socle, because the socle, the foundations, and the flooring do not have thermal insulation. Comparable problematic situation is presented by Al-Anzi and Krarti (2004). Another problem with the uninsulated structure is at the top part of the gable wall. Problematic structure here is the steel concrete straining band of the outer wall without thermal insulation. This layer is located under the steel concrete roof frame. These thermal defects of the envelope are comparable to the results presented by Höglund and Burstrand (1998); Fukuyo (2003); Juárez et al. (2012); and Al-Sanea and Zedan (2012).

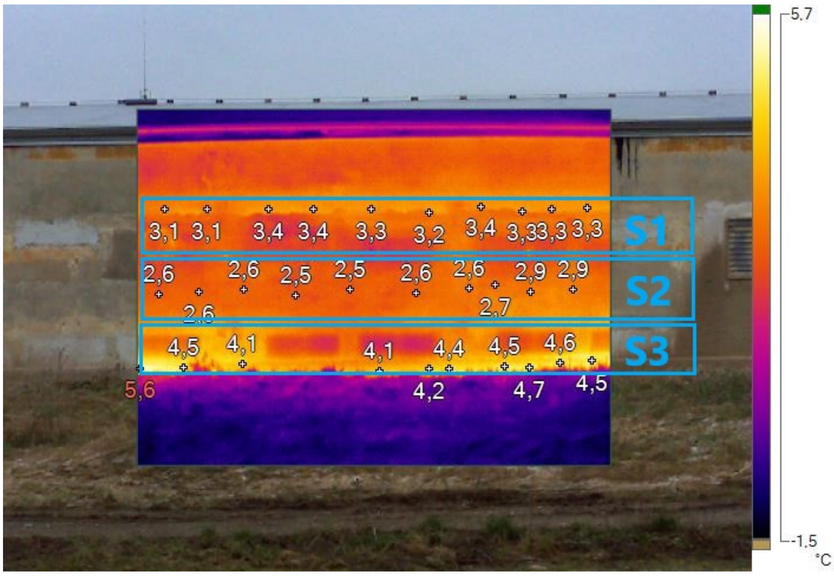

Fig. 1 Thermogram of the poultry house façade

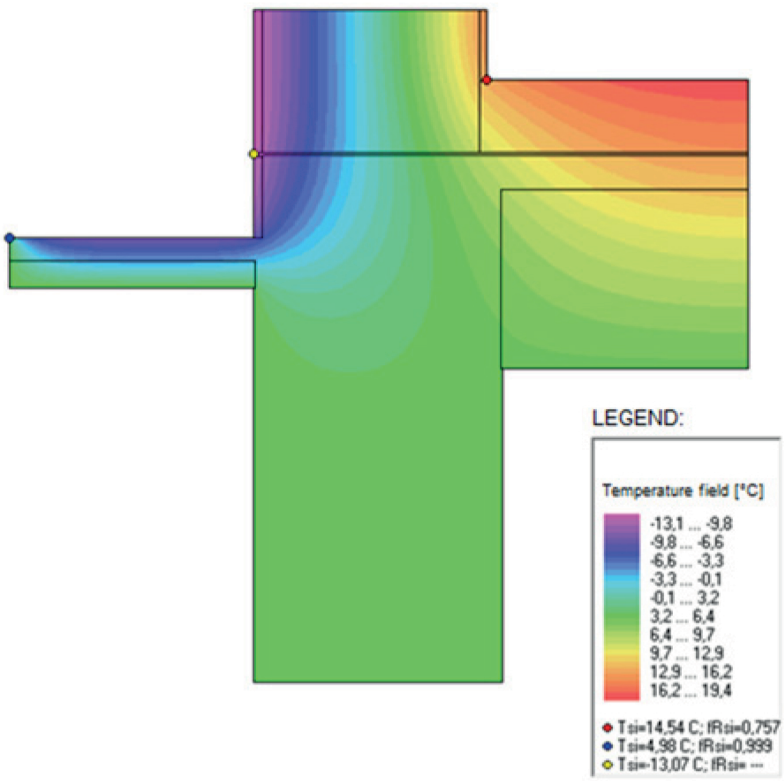

Fig. 2 Computer model of temperature field of the detail at the critical point of socle part of the wall, foundation structures, and thermally uninsulated floor of the poultry house structure

The most problematic of this structure is the straining band and uninsulated socle. Figure 1 represents the thermograms of the poultry house with similar situation, confirming the inappropriate technical design of structure details. The surface temperatures of the measured structure in Fig. 1 are +1.4 °C (t_{min}) +5.6 °C (t_{max}). The temperature field model is shown in Fig. 2.

Table 1 shows that the differences between the medians and means of the individual datasets are not large. The variability is higher compared to the datasets presented in the other chapters. The hypothesis of a normal distribution of the data was rejected in the case of datasets S2 and S3. Data set S3 is significantly peaked and skewed.

Regarding the results of the exploratory analysis, non-parametric tests were used for the purpose of inter-comparison. From the results presented in Table 2, the hypothesis of a statistically insignificant difference between the measured values was rejected at the $\alpha = 0.05$ level of significance.

Table 2 Post-hoc statistical analysis of observed values for a typical thermogram of the poultry house structure

Test area	Nemenyi *p*-value	Dunn *p*-value
S2-S1	0.0298	0.0214
S3-S1	0.0298	0.0107
S3-S2	1.1E-06	0.0000009

Table 1 Descriptive statistics of the analysed areas of a typical thermogram of the poultry house structure

Area	Mean (°C)	Median (°C)	SD (°C)	IQR (°C)	Variation coefficient	Skewness	Kurtosis	S-W
S1	3.28	3.3	0.113529	0.15	0.034613	-0.660623	-0.708977	0.0553
S2	2.65	2.6	0.143372	0.075	0.054103	1.1310581	0.2385474	0.01123
S3	4.52	4.5	0.431535	0.325	0.095472	1.8723759	4.6889288	0.01344

SD – standard deviation; IQR – interquartile range; S-W – Shapiro-Wilk test

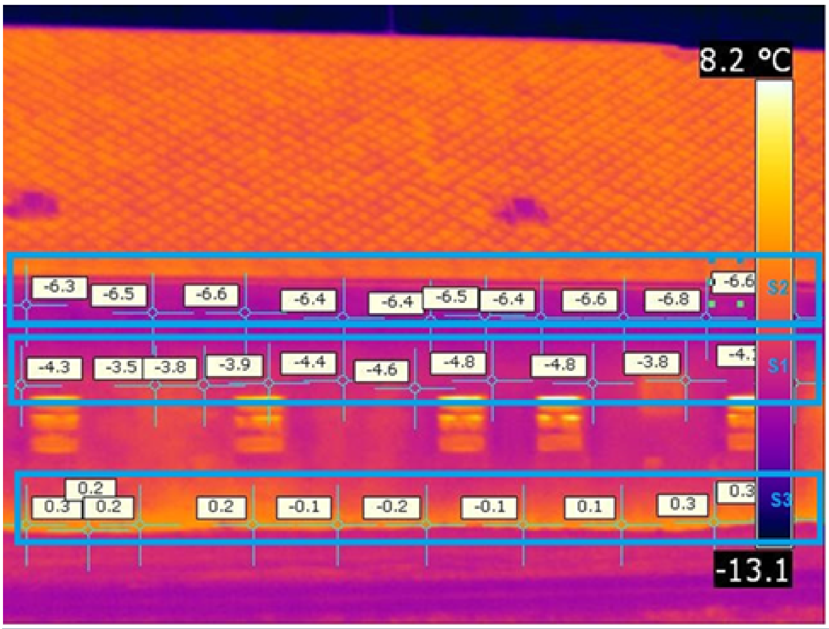

Fig. 3 Thermogram of the piggery façade

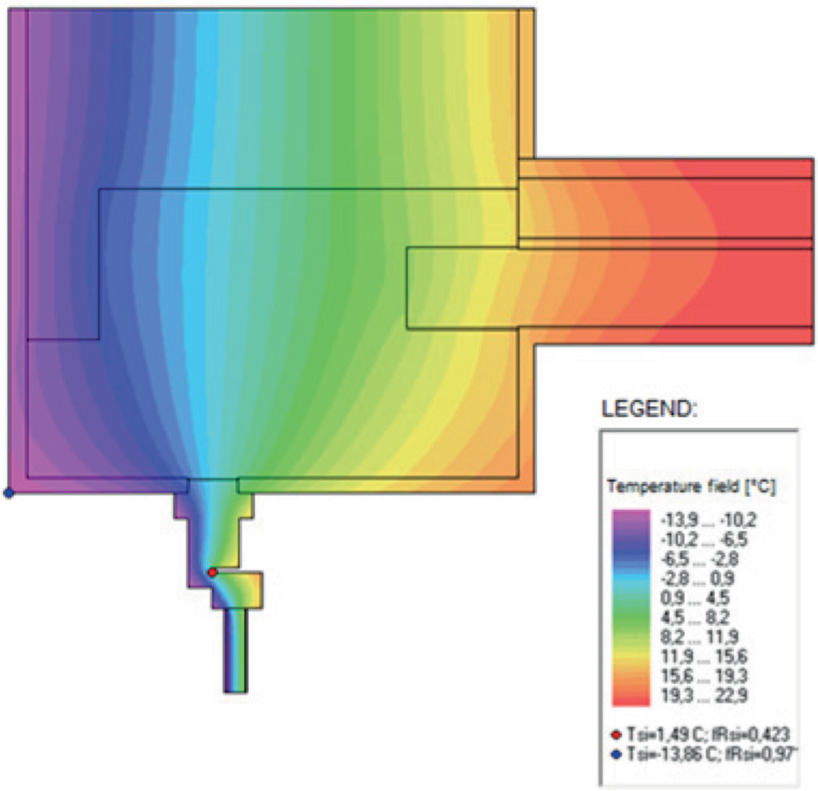

Fig. 4 Computer model of the temperature field of the detail at the point of transition of vertical support structures to horizontal support and stiffening structures of the piggery

Case study 2 – old piggery

The second object for IR thermography survey is an old piggery. The thermographic measurement was made under the following boundary conditions: internal temperature t_i = 22 °C; external air temperature t_e = -8.8 °C; relative humidity 83%; the distance of the measured object 20.7 m; air velocity v_a = 0.40 m·s^{-1}; and emissivity 0.92.

In a typical thermogram shown in Fig. 3, areas are delineated, from which surface temperature values are subsequently taken for further evaluation. The individual areas are labelled in the thermogram and can be specified as follows: Area S1 (numerous temperature anomalies at the reinforced concrete ring beam); Area S2 (hall façade without significant temperature anomalies); Area S3 (numerous temperature anomalies at the floor structure and socle). The surface temperatures of the measured structure in Fig. 3 are -7.3 °C (t_{min}) +6.1 °C (t_{max}). The temperature field model and construction layout of the critical lintel detail and reinforced ring beam are shown in Fig. 4.

Table 3 presents the results of the exploratory analysis. From the data presented in Tables 3 and 4, the hypothesis of normal distribution of data in datasets S1, S2, and S3 was not rejected.

Table 4 Test of homogeneity of the variance of observed values for a typical thermogram of the piggery façade

Type of test	*p*-value
Bartlett	0.001859
Leven	0.00764

Table 3 Descriptive statistics of the analysed areas of typical thermogram of the piggery façade

Area	Mean (°C)	Median (°C)	SD (°C)	IQR (°C)	Skewness	Kurtosis	S-W
S1	-4.22	-4.3	0.451664	0.725	0.1541144	-1.246247	0.4616
S2	-6.51	-6.5	0.144914	0.2	-0.607915	0.4383976	0.4851
S3	0.12	0.2	0.18738	0.325	-0.739716	-1.07409	0.0494

Table 5 Post-hoc statistical analysis of the observed values for a typical thermogram of the piggery façade

Test area	Nemenyi *p*-value	Dunn *p*-value	ANOVA (Tukey) *p*-value
S2-S1	0.0298	0.0218	<2e-16
S3-S1	0.0298	0.0109	<2e-16
S3-S2	1.1E-06	1.06E-06	<2e-16

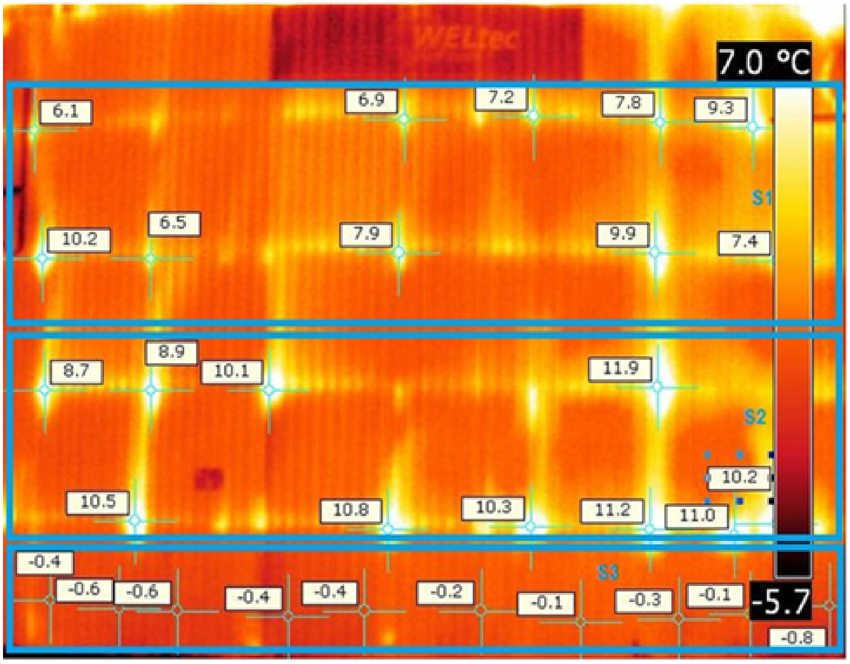

Fig. 5 Thermogram of the farm biogas plant – the fermenter envelope

However, the hypothesis of the homogeneity of variance was rejected at the specified significance level. For testing the hypothesis of statistically significant differences between the data sets, both parametric and non-parametric tests were used. As seen in the results in Table 5, the hypothesis was rejected in all the cases.

Case study 3 – farm biogas plant

The third object for IR thermography survey is a farm biogas plant. The thermographic measurements were carried out under the following boundary conditions: fermenter operating temperature t_i = 40 °C; outdoor air temperature t_e = -8.8 °C; relative humidity 82%; the distance of the measured object 15.3 m; air velocity v_a = 0.40 m·s^{-1}; and emissivity 0.84.

Figure 5 shows a typical thermogram of the fermenter envelope. Numerous systematic thermal bridges can be seen, mainly formed by the supporting grating of steel thin-walled sections anchored to the actual corrosion-resistant steel tank. The grating is made in a 1.0 m grid and is hidden behind an outer cladding of painted steel trapezoidal sheets. Thermal insulation boards made

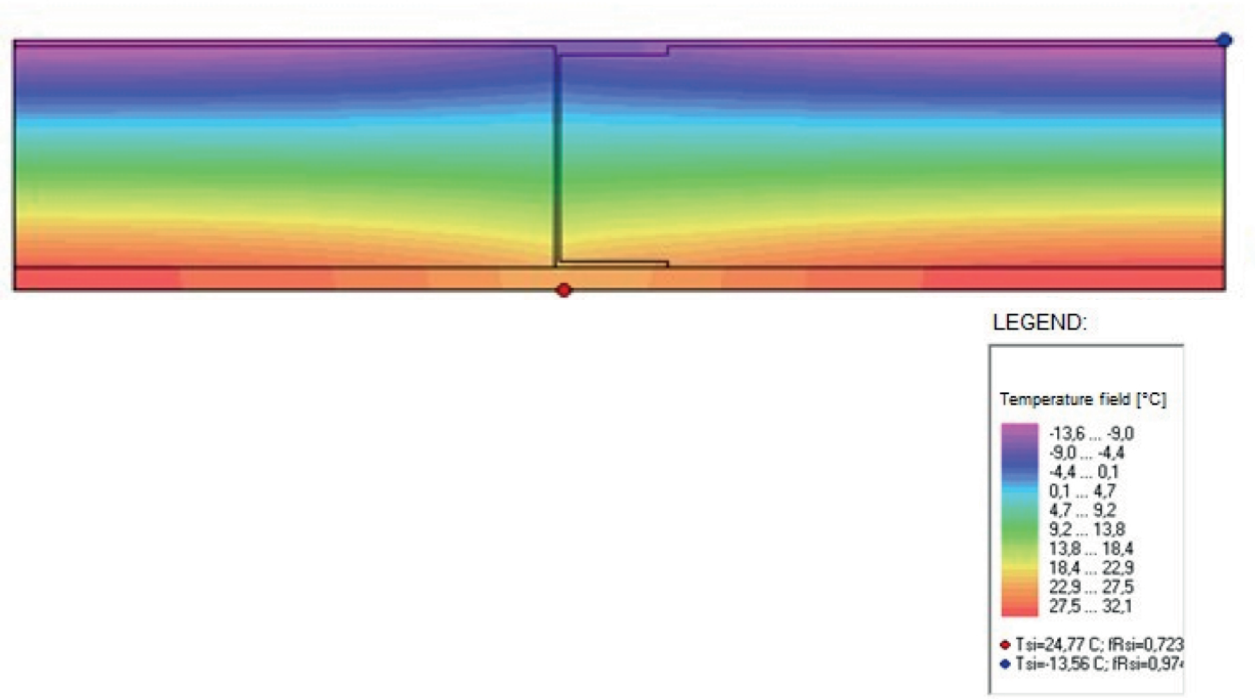

Fig. 6 Computer model of the temperature field of the cross-sectional detail of the fermenter wall envelope

Table 6 Descriptive statistics of the analysed areas of a typical thermogram of the farm biogas plant – the fermenter envelope

Area	Mean (°C)	Median (°C)	SD (°C)	IQR (°C)	Variation coefficient	Skewness	Kurtosis	S-W
S1	7.92	7.6	1.421892	1.975	0.179532	0.5688494	-1.0031	0.341
S2	10.36	10.4	0.982288	0.825	0.094815	-0.456215	-0.009354	0.6287
S3	-0.39	-0.4	0.228279	0.325		-0.362872	-0.508649	0.5572

of polystyrene foam are placed between the individual grid profiles. As there is no interruption of the heat flow between the fermenter and the grating structure, there is a direct heat transfer from the heated fermenter to the outer sheet metal cladding and thus higher heat losses. The higher surface temperatures (t_s = 7.6 °C and t_s = 9.8 °C respectively) at the locations of this systematic thermal bridge only confirm the incorrect design of this construction detail. As can be seen, the highest surface temperatures are achieved at the intersection of the vertical and horizontal steel sections of the grating, probably because the welds at these points are anchored directly to the tank. The temperature field model is shown in Fig. 6.

In a typical thermogram shown in Fig. 5, areas are delineated, from which surface temperature values are then taken for further analysis. The delineated areas are shown schematically in the thermogram and include the points under consideration with their respective temperature values. The individual surfaces are labelled in the thermogram and can be specified as follows: surface S1 (numerous temperature anomalies in the location of the concealed supporting steel frame with anchoring and cladding with riveted profiled plates); surface S2 (numerous temperature anomalies in the location of the concealed supporting steel frame with anchoring and cladding with riveted profiled plates); and surface S3 (fermenter shell without significant temperature anomalies). From Table 6, the hypothesis of normal distribution of data sets S1, S2, and S3 was not rejected in any case. On the other hand, the coefficient of variation suggests that the variability of data is relatively high. To test the assumptions for the use of ANOVA, a homogeneity of variances test was performed. For this purpose, Bartlett's test and Levene's test were used. In both cases, the hypothesis of homogeneity of variances was rejected.

Considering the prerequisites for the use of parametric tests were not met, a non-parametric test was performed. From the results below, in the case of S2 and S1 area, the hypothesis was not rejected in Nemenyi test, whereas in the case of Dunn test, the hypothesis was rejected. However, both values are close to the statistical significance level of $\alpha = 0.05$. For further decision making, a one-factor ANOVA was also used. The resulting *p*-value was well below the statistical significance level, and the hypothesis was rejected. Based on the median values of datasets S1 and S2 and considering the large variability in the data and the results of the above tests, the authors are inclined to decide that there is a statistically significant difference between datasets S1 and S2.

From the typical thermograms, the computer models of temperature fields and detailed analysis of the design of critical points in the case studies, it is evident that significant systematic and point thermal bridges occur in older and modern heated agricultural building designs. Characteristic thermal engineering defects include the details at the point of the masonry socle and the transition of the floor structure to the vertical masonry creating a significant thermal bridge. This is due to an insufficient thermal insulation of the foundation structure and socle masonry. It is also due to the insufficient thickness of the thermal insulation of concrete floor structures. Especially in the floor structure, the absence of the intensive thermal insulation layer has a significant impact on high heat losses due to the installed underfloor hot water heating, which transfers heat to the floor structure, from where it spreads to the surrounding structures. Comparable thermal engineering problems are reported by Al-Anzi and Krarti, 2004).

The suitability of combining the IRT and computer simulation methods in assessing the details of building structures is demonstrated in a comparative work by Cappelletti et al. (2011). Significant thermal anomalies are evident in some areas of the building envelope due to the reduction of thickness of the masonry structure or the existence of walled steel structures with high thermal conductivity (past building modifications). In biogas plants, it is evident that there are numerous systematic thermal bridges, mainly consisting of a supporting grating of thin-walled steel sections anchored to the corrosion-resistant steel tank itself. Comparable defects in the envelope of old buildings and the relevance of sufficient thermal insulation properties of structures are presented by Al-Hamoud (2005). Similar thermal bridges in building envelope structures and their effect on the thermal protection of buildings are presented by Theodosiou et al. (2021) and Larbi (2005).

Another critical detail is reinforced concrete ring beams. This layer runs around the perimeter of buildings situated under the roof structure, which has insufficient thermal insulation properties. The thermal bridge at the location of the supporting steel roof frames on the supporting masonry is related to this critical detail. A comparable problem is reported by Höglund and Burstrand (1998); Juárez et al. (2012); Al-Sanea and Zedan (2012); and Taylor et al. (2014).

Another critical detail evident in the thermograms is the frames of the windows, doors, and gates, especially at the point of connection to the perimeter masonry. This unsatisfactory condition is probably due to the poor design of the connection joints between the frames and the perimeter masonry, where there is no insulation layer to break the heat flow. Similar findings for the critical details of the connection between the masonry and the window and door frames are published by Ben-Nakhi (2002) and Cappelletti et al. (2011). A comparable problem of the thermal bridges caused by reinforced concrete ring beams is presented by Fukuyo (2003).

Conclusion

The results of experimental thermographic measurements and computational evaluations of the envelopes of selected agricultural heated buildings have shown the occurrence of several thermal technical faults that directly affect the energy consumption and have an impact on the proper function and durability of the building materials of the envelope structures. The results of the computer modelling of temperature fields in the critical construction details as well as a detailed analysis of the typical thermograms for each of the agricultural buildings proved the existence of significant thermal anomalies due to an inappropriate structural design.

Temperature field diagrams in the critical detail indicate intense heat flux and a high risk of water vapour condensation due to temperature reduction below the dew point. Intense heat flux at critical points is documented in the thermograms. Temperature anomalies were found especially in the details of the building envelope, horizontal and floor structures. The utilisation of the information presented in this paper on the systematic thermal engineering defects of the envelope, identified by experimental IRT measurements and computer modelling, can be found in the design of new buildings or reconstruction of older buildings. The assessment of heat flow is an evaluation criterion of the quality of building design, which is directly reflected in annual energy consumption required to cover the heat loss through the building envelope of the assessed building. The aim is to properly design the construction junctions so that the negative thermal bridge effect is reduced to a negligible impact, which implicitly provides reduced energy consumptions while respecting the relevant legislative requirements.

References

AL-ANZI, A. – KRARTI, M. 2004. Local/global analysis of transient heat transfer from building foundations. In Building and Environment, vol. 39, no. 5, pp. 495–504. DOI: https://doi.org/10.1016/j.buildenv.2003.10.003

AL-HOMOUD, M. S. 2005. Performance characteristics and practical applications of common building thermal insulation materials. In Building and Environment, vol. 40, no. 3, pp. 353–366. DOI: https://doi.org/10.1016/j.buildenv.2004.05.013

Al-SANEA, S. A. – ZEDAN, M. F. 2012. Effect of thermal bridges on transmission loads and thermal resistance of building walls under dynamic conditions. In Applied Energy, vol. 98, pp. 584–593. DOI: https://doi.org/10.1016/j.apenergy.2012.04.038

BALARAS, C. A. – ARGIRIOU, A. A. 2002. Infrared thermography for building diagnostics. In Energy and Buildings, vol. 34, no. 2, pp. 171–183. DOI: https://doi.org/10.1016/S0378-7788(01)00105-0

BEN-NAKHI, A. E. 2002. Minimizing thermal bridging through window systems in buildings of hot regions. In Applied Thermal Engineering, vol. 22, no. 9, pp. 989–998. DOI: https://doi.org/10.1016/S1359-4311(01)00121-1

CAPPELLETTI, F. – GASPARELLA, A. – ROMAGNONI, P. – BAGGIO, P. 2011. Analysis of the influence of installation thermal bridges on windows performance: The case of clay block walls. In Energy and Buildings, vol. 43, no. 6, pp. 1435–1442. DOI: https://doi.org/10.1016/j.enbuild.2011.02.004

EL SAIED, A. – MAALOUF, C. – BEJAT, T. – WURTZ, E. 2022. Slab-on-grade thermal bridges: A thermal behavior and solution review. In Energy and Buildings, vol. 257, article no. 1111770. DOI: https://doi.org/10.1016/j.enbuild.2021.111770

EN ISO 10211:2020. Thermal bridges in building construction – Heat flows and surface temperatures – Detailed calculations.

EN 13187:1999. Thermal performance of buildings – Qualitative detection of thermal irregularities in building envelopes – Infrared method.

FUKUYO, K. 2003. Heat flow visualization for thermal bridge problems. In International Journal of Refrigeration, vol. 26, no. 5, pp. 614–617. DOI: https://doi.org/10.1016/S0140-7007(03)00006-9

GE, J. – XUE, Y. – FAN, Y. 2021. Methods for evaluating and improving thermal performance of wall-to-floor thermal bridges. In Energy and Buildings, vol. 231, article no. 110565. DOI: https://doi.org/10.1016/j.enbuild.2020.110565

HERBUT, P. – RZEPCZYŃSKI, M. – ANGRECKA, S. 2018. The analysis of efficiency and investment profitability of a solar water heating system in a multi-family building. In Journal of Ecological Engineering, vol. 19, no. 6, pp. 75–80. DOI: https://doi.org/10.12911/22998993/92675

HÖGLUND, T. – BURSTRAND, H. 1998. Slotted steel studs to reduce thermal bridges in insulated walls. In Thin-Walled Structures, vol. 32, no. 1–3, pp. 81–109. DOI: https://doi.org/10.1016/S0263-8231(98)00028-7

CHANGMIN, K. – GWANYONG, P. – HYANGIN, J. – EUI-JONG, K. 2022. Automated classification of thermal defects in the building envelope using thermal and visible images. In Quantitative InfraRed Thermography Journal, vol. 20, no. 3, pp. 106–122. DOI: https://doi.org/10.1080/17686733.2022.2033531

CHEN, X. – SHUAI, C. – ZHANG, Y. – WU, Y. 2020. Decomposition of energy consumption and its decoupling with economic growth in the global agricultural industry. In Environmental Impact Assessment Review, vol. 81, article no. 106364. DOI: https://doi.org/10.1016/j.eiar.2019.106364

CHOI, J.-S. – KIM, C. – JANG, H. – KIM, E.-J. 2022. Dynamic thermal bridge evaluation of window-wall joints using a model-based thermography method. In Case Studies in Thermal Engineering, vol. 35, article no. 102117. DOI: https://doi.org/10.1016/j.csite.2022.102117

JUÁREZ, M. C. – MORALES, M. P. – MUŇOZ, P. – MENDÍVIL, M. A. 2012. Influence of horizontal joint on the thermal properties of single-leaf walls with lightweight clay blocks. In Energy and Buildings, vol. 49, pp. 362–366. DOI: https://doi.org/10.1016/j.enbuild.2012.02.033

KARAS, I. – GÁLIK, R. 2004. Contact and non-contact thermometry in the milking acquisition process. In Czech Journal of Animal Science, vol. 49, no. 1, pp. 1–7. DOI: https://doi.org/10.17221/4264-CJAS

KEMPTON, L. – KOKOGIANNAKIS, G. – GREEN, A. – COOPER, P. 2021. Evaluation of thermal bridging mitigation techniques and impact of calculation methods for lightweight steel frame external wall systems. In Journal of Building Engineering, vol. 43, article no. 102893. DOI: http://dx.doi.org/10.1016/j.jobe.2021.102893

KIM, S. – SEO, J. – JEONG, H. – KIM, J. 2022. In situ measurement of the heat loss coefficient of thermal bridges in a building envelope. In Energy and Buildings, vol. 256, article no. 111627. DOI: https://doi.org/10.1016/j.enbuild.2021.111627

KYTHREOTOU, N. – FLORIDES, G. – TASSOU, S. A. 2012. A proposed methodology for the calculation of direct consumption of fossil fuels and electricity for livestock breeding, and its application to Cyprus. In Energy, vol. 40, no. 1, pp. 226–235. DOI: https://doi.org/10.1016/j.energy.2012.01.077

LARBI, A. B. 2005. Statistical modelling of heat transfer for thermal bridges of buildings. In Energy and Buildings, vol. 37, no. 9, pp. 945–951. DOI: https://doi.org/10.1016/j.enbuild.2004.12.013

MAYER, Z. – KAHN, J. – HOU, Y. – GÖTZ, M. – VOLK, R. – SCHULTMANN, F. 2023. Deep learning approaches to building rooftop thermal bridge detection from aerial images. In Automation in Construction, vol. 146, article no. 104690.
DOI: https://doi.org/10.1016/j.autcon.2022.104690

TAYLOR, T. – COUNSELL, J. – GILL, S. 2014. Combining thermography and computer simulation to identify and assess insulation defects in the construction of building façade. In Energy and Buildings, vol. 76, pp. 130–142. DOI: https://doi.org/10.1016/j.enbuild.2014.02.080

TEJEDOR, B. – BARREIRA, E. – ALMEIDA, R. M. S. F. – CASALS, M. 2020. Thermographic 2D U-value map for quantifying thermal bridges in building façades. In Energy and Buildings, vol. 224, article no. 110176. DOI: https://doi.org/10.1016/j.enbuild.2020.110176

THEODOSIOU, T. – TSIKALOUDAKI, K. – KONTOLEON, K. – GIARMA, C. 2021. Assessing the accuracy of predictive thermal bridge heat flow methodologies. In Renewable and Sustainable Energy Reviews, vol. 136, article no. 110437.
DOI: https://doi.org/10.1016/j.rser.2020.110437

VITÁZEK, I. – TIROL, J. 2008. Relation between surface temperature and dryer operation. In Research in Agricultural Engineering, vol. 54, no. 4, pp. 176–182. DOI: https://doi.org/10.17221/14/2008-RAE

VÍTĚZ, T. – TRÁVNÍČEK, P. 2011. The measurement of heat loss with use of a thermal imaging system. In Acta Universitatis Agriculturae et Silviculturae Mendelianae Brunensis, vol. 59, no. 3, pp. 193–196. DOI: https://doi.org/10.11118/actaun201159030193

XUE, Y. – FAN, Y. – CHEN, S. – WANG, Z. – GAO, W. – SUN, Z. – GE, J. 2023. Heat and moisture transfer in wall-to-floor thermal bridges and its influence on thermal performance. In Energy and Buildings, vol. 279, article no. 112642.
DOI: https://doi.org/10.1016/j.enbuild.2022.112642

ZHAO, K. – JIANG, Z. – HUANG, Y. – SUN, Z. – WANG, L. – GAO, W. – GE, J. 2022. The method of reducing heat loss from thermal bridges in residential buildings with internal insulation in the hot summer and cold winter zone of China. In Journal of Building Engineering, vol. 62, article no. 105421. DOI: https://doi.org/10.1016/j.jobe.2022.105421